SYNTHESIS, STRUCTURAL AND OPTICAL STUDIES OF PdS NANOCRYSTALS AND PdS/STARCH NANOCOMPOSITES FROM DITHIOCARBAMATE SINGLE SOURCE PRECURSORS

P. A. AJIBADE[a*], A. NQOMBOLO[b]
[a]*School of Chemistry and Physics, University of KwaZulu-Natal, Pietermaritzburg campus, Private Bag X01, Scottsville 3209, South Africa;*
[b]*Department of Chemistry, University of Fort Hare, Private Bag X1314, Alice 5700, South Africa*

We report the synthesis of PdS nanocrystals and PdS/potato starch nanocomposites using dithiocarbamate single source precursor's thermolysed in hexadecylamine. The optical studies of the nanoparticles showed that the absorption spectra of the PdS nanoparticles are blue shifted compared to their corresponding bulk materials while the photoluminescence spectra show narrow emissions that are red-shifted. The XRD patterns confirmed the formation of cubic phase for PdS nanoparticles. TEM images of PdS showed monodisperse nanocrystals with average crystallite sizes of 6.94-9.62 nm for **PdS1**, 4.94-6.52 for **PdS2**, and 7-10.43 for **PdS3.** The SEM images showed uniform surface morphology of PdS nanoparticles with almost spherically shaped nanoparticles, while EDS confirms the presence of Pd and S for HDA-capped PdS nanoparticles. SEM images and EDS of the PdS/potato starch nanocomposites confirmed the dispersion of the nanoparticles in starch matrices and their FTIR further confirms interactions between the PdS nanocrystals and the starch matrices in the nanocomposites.

(Received November 18, 2017; Accepted December 8, 2018)

Keywords: Dithiocarbamate; PdS; Nanoparticles; Starch; Nanocomposites; Morphology

1. Introduction

Nanoparticles have been the subject of intense investigations in recent years because of their unique properties, which are strongly dependant on the materials composition, shapes and sizes [1, 2]. II–VI semiconductor nanocrystals are of interest because of their size-dependant properties compared with those of bulk materials [3-7]. Different methods such as sputtering [8, 9], co-precipitation [10], sol gel [11], micro emulsion [12], hydrothermal [13] or single source precursor [14] are used for the synthesis of nanoparticles. The use of single source precursors for the synthesis of thin films and nanocrystals has been an area of intense research [14, 15]. The use of single-source molecular precursors in which the metal-chalcogenide bond is available has served as efficient route to improve quality and produce crystalline monodispersed nanoparticles of semiconducting materials [16-24].

Among chalcogenides complexes, the compounds that have found greatest use as precursors for II–VI semiconductors are the dithiocarbamate complexes [19-24]. Thermolysis of single source precursor in high boiling point solvents produces nanocrystals with narrow size distribution [25-28], and recent studies have shown that variation of thermolysis temperatures, precursor concentrations and time may lead to the formation of nanocrystalline materials with different shapes and sizes [29-31]. In this research, we are interested in investigating the optical and structural properties of HDA capped PdS nanocrystals prepared from homoleptic Pd(II) dithiocarbamate single source molecular precursors. The choice of HDA as a preferred capping agent in this work arose from the fact that it is an effective capping agent with good selectivity [32]. It decreases the growth rate, size of nanoparticles and improves the photoluminescence quantum efficiency by effectively passivating the surface defects while behaving as non-

* Corresponding author: ajibadep@ukzn.ac.za

radioactive relaxing centre. These properties attributed to its high electron donating ability and capping density because of its small stereochemical interference [33, 34]. The optical properties of the nanocrystals were studied using absorption and photoluminescence spectroscopy while scanning electron microscopy (SEM), X-ray dispersive spectroscopy (EDS), transmission electron microscopy (TEM) and X-ray diffraction (XRD) techniques were used to study their structural properties.

2. Experimental

2.1. Materials and physical measurements

All chemicals and reagents used were of analytical grade and used as obtained without further purification. The potassium salt of the dithiocarbamate were prepared by methods reported in the literature [35]. $Pd(CH_3CN)_2]$ was prepared by literature method [36] and the palladium complexes were also prepared and characterized as reported in the literature [37]. A Perkin Elmer Lambda 25 UV–Vis spectrophotometer was employed to carry out optical measurements at room temperature. The photoluminescence of the nanoparticles were measured using Perkin Elmer LS 45 fluorimeter. Powder X-ray diffraction patterns were recorded on Bruker-D8 advance powder X-Ray diffractometer instrument operating at a voltage of 40 kV and a current of 30 mA with Cu Kα radiation. The X-ray diffraction data were analysed using EVA (evaluation curve fitting) software. The phase identification was carried out with the help of standard JCPDS database. The transmission electron microscopy (TEM) images were obtained using a ZEISS Libra 120 electron microscope operated at 120 kV. The samples were prepared by placing a drop of a solution of the sample in toluene on a carbon coated copper grid (300 mesh, agar). Images were recorded on a mega view G2 camera using iTEM Olympus software. The scanning electron microscopy (SEM) images were obtained on a Joel, JSM-6390 LV apparatus, using an accelerating voltage between 15-20 kV at different magnifications. Energy dispersive spectra were processed using energy dispersive X-ray spectroscopy (EDS) attached to a Joel, JSM-6390 LV SEM with Noran system Six software [32, 35].

2.2 Preparation of the PdS nanoparticles

0.40 g of the respective metal precursor was dissolved in 4 mL of trioctylphosphine (TOP) and injected into 3 g of hot hexadecylamine 220 ^{o}C. A constant temperature was maintained for a period of 1 hr under the flow of nitrogen while stirring [35]. The mixture was cooled to room temperature and excess methanol was added to precipitate the nanoparticles and remove excess HDA. The precipitates were separated by centrifugation and washed with methanol and the resulting solid precipitates of HDA capped PdS nanoparticles were dried at room temperature.

3. Results and discussion

3.1. Optical properties of the nanoparticles

The energy band gap is the main optical property of semiconductor nanoparticles. Figure 1 shows the UV-Vis absorption spectra of PdS nanoparticles. The absorption band edges of the PdS nanoparticles were found to be 324, 318 and 326 nm and their calculated band gaps were found to be 3.87, 3.94, and 3.84 eV. These are found to be blue shifted relative to the bulk (2.0 eV) and shows they have small particle size ascribe to the quantum confinement effect [38]. The photoluminescence (PL) spectra (Figure 2) of the PdS nanoparticles show emission close to the absorption band edges. The emission maximum of the PdS nanoparticles appear at 710, 714, and 377 nm for PdS1, PdS2, and PdS3 respectively. These emission peaks were also found to be red shifted relative to the optical absorption band edges. The emission maxima show red shift and is consistent with the blue shifts observed in the absorption spectra. The emission peaks showed the monodispersed nature of the PdS nanoparticles [39].

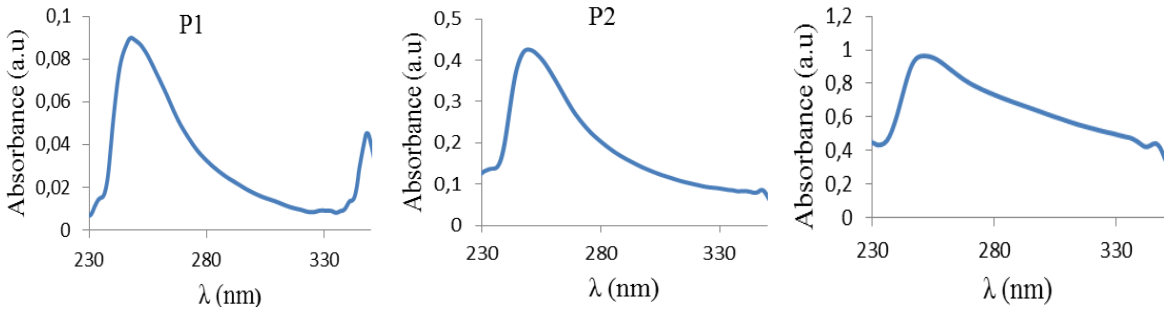

Fig. 1. UV-Vis absorption spectra of HDA-capped PdS nanoparticles

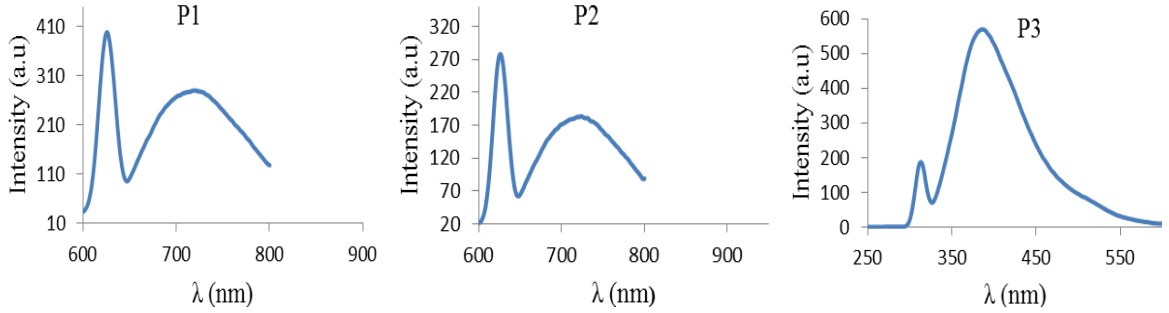

Fig. 2. PL spectra of HDA-capped of PdS nanoparticles

3.2. X-ray diffraction studies of the PdS nanoparticles

Fig. 3 shows the XRD diffraction patterns for the PdS nanoparticles. The XRD patterns of PdS1 shows three peaks at 2θ values around 19.9, 21.7 and 23.1 which corresponds to (002), (100) and (110) Miller indices for cubic PdS nanoparticles. The broadness of the peaks is the indication of small particle size. The elongation of the XRD pattern is the confirmation that an organic capping agent (HDA) was used in the synthesis of the nanoparticles [39, 40].

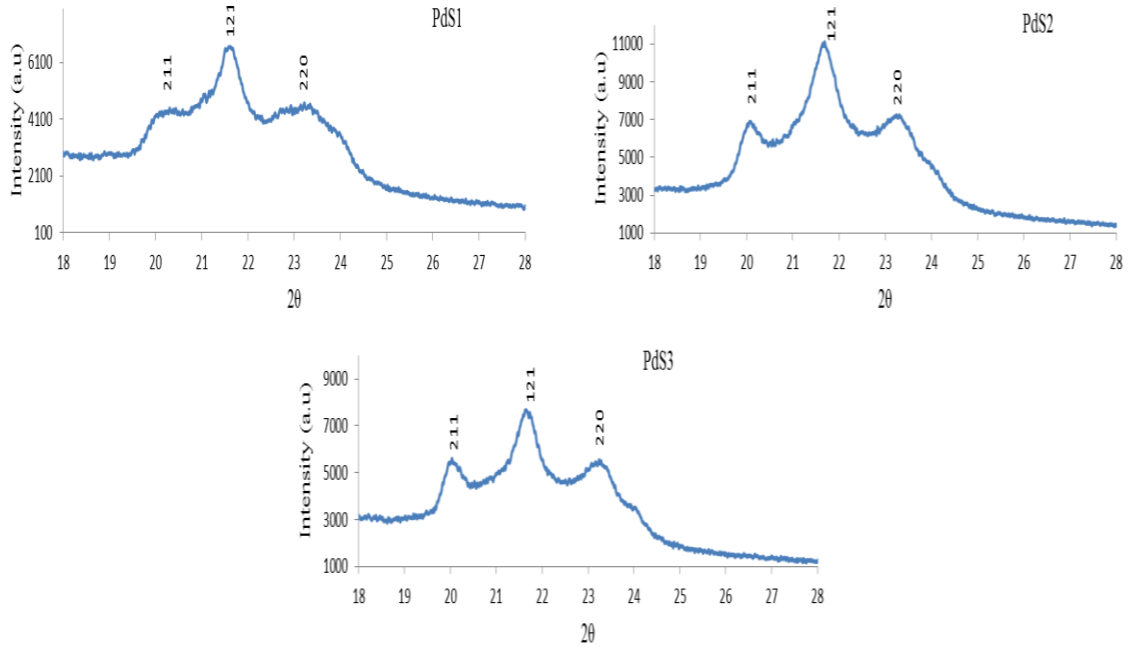

Fig. 4. XRD patterns of HDA-capped PdS nanoparticles

3.3. TEM studies palladium sulfide nanoparticles

Fig. 4 shows TEM images of HDA-capped PdS prepared at 220 °C. Figure 4(A) shows TEM images of HDA-capped PdS1 nanoparticles with spherical shapes with very small size ranging from 6.94-9.62 nm. There is no agglomeration of particles because the precursor was perfectly capped with the HDA [41]. PdS2 nanoparticles (Fig. 4B) show close to spherical shape with uniform size distribution with particle sizes ranges from 4.72-6.84 nm. Figure 4C shows PdS3 nanoparticles with spherical shape and size distribution of 7.15-16.46 nm. The particles are well dispersed and there are no aggregation and this is an indication of strong bonding of dithiocarbamate ligands onto the metal ion [40]

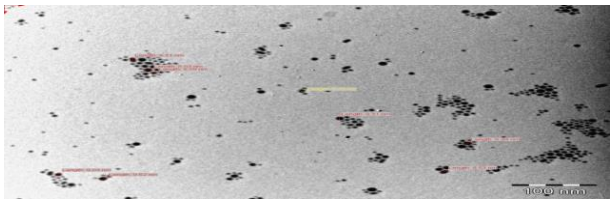

a)

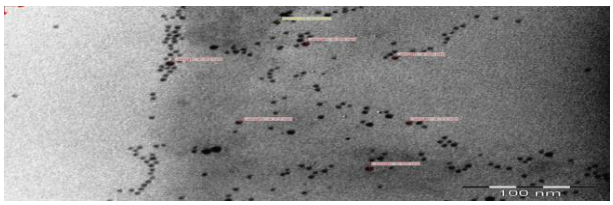

b)

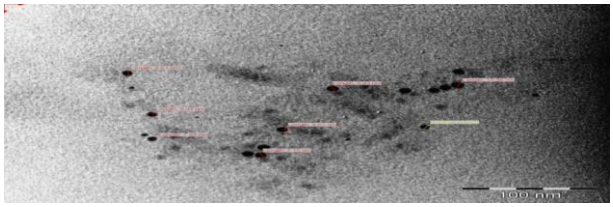

c)

*Fig. 4. TEM images of PdS nanoparticles (A): PdS**1** from Complex 1, (B): PdS**2** from complex 2 and (C): PdS**3** from complex 3*

3.4 Morphological studies of the nanoparticles

The SEM images of the synthesized HDA-capped PdS nanoparticles are shown in Figure 5 labelled A (low magnification) and B (high magnification). The results show that PdS1 has homogeneous surface morphology and is smooth. In both high and low magnification, they have pores in between particles and these nanoparticles do not aggregate [42]. EDS for the analysis of elemental composition was done and the spectrum is labelled C. From the obtained results from EDS, Pd and S are present and this confirms the formation of PdS nanoparticles. Other traces of elements such as C, O, and P are also observed. The observed C is attributed to carbon of the capping agent (HDA), P is due to TOP, and O might be due to the oxidation of sulfur to oxygen atoms [43]. SEM images of PdS2 nanoparticles prepared from $[Pd(L^2)_2]$ precursor complex are shown on Figure 6 with the same surface morphology and close to spherical shape. Figure 6C show EDS spectrum with both Pd and S present. P is due to TOP and C is due to the capping agent (HDA). SEM images of PdS3 nanoparticles are shown in Figure 7. The surface is rougher with hollow like structures [44]. These nanoparticles have uniform surface morphology and there are no lumps. From the EDS analysis, both elements are present and P is due to the TOP used and the observe C is from the HDA capping agent.

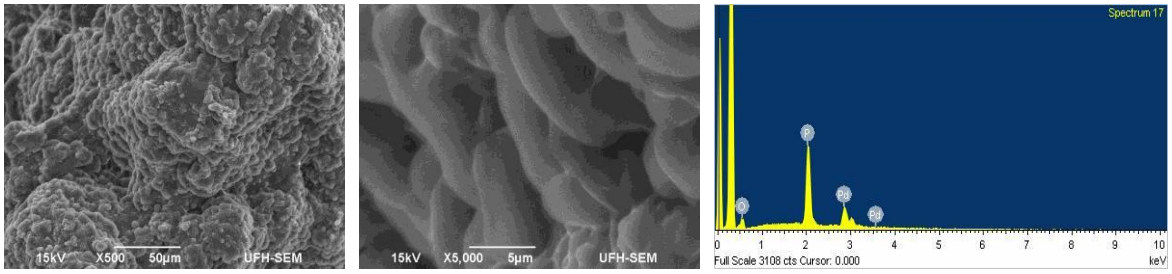

Fig. 5. SEM images of PdS1 (A) low mag (B) high mag (C) EDS spectrum of the sample

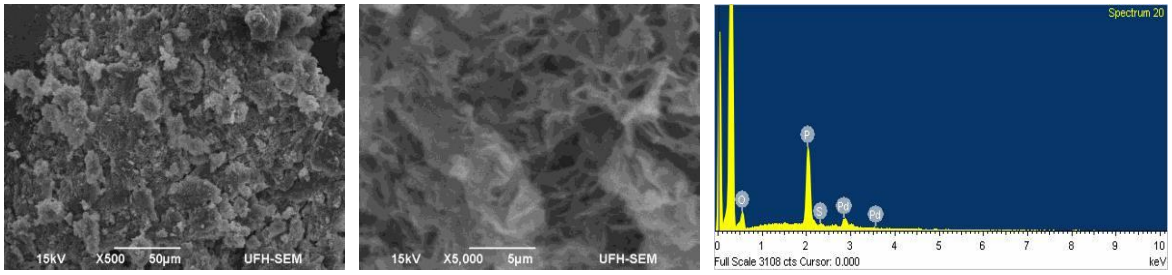

Fig. 6. SEM images of PdS from [Pd(L^2)$_2$] complex (D) low mag (E) high mag (F) EDS spectrum of the sample

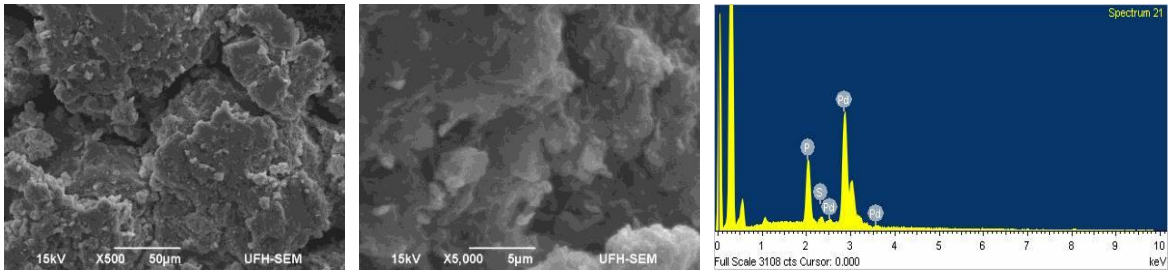

Fig. 7. SEM images of PdS from [Pd(L^3)$_2$] complex (G) low mag (H) high mag (I) EDS spectrum of the sample

3.5 Structural studies of PdS/starch nanocomposites

SEM images of PdS1/starch polymer nanocomposites are shown on Figure 8 (A) low magnification and (B) high magnification. Image A show dispersed nanoparticles that are on the surface of potato starch polymer. There is an increase in the surface roughness of the particles [45].

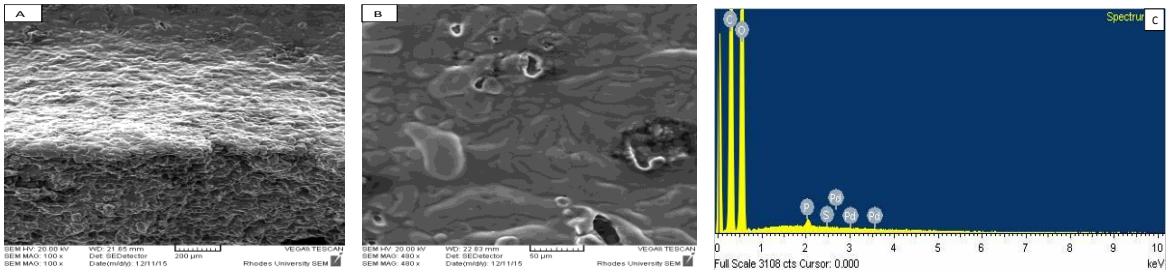

Fig. 8. (A) and (B) are SEM images of PdS1/potato starch nanocomposites. (C) EDS spectrum of the nanocomposites

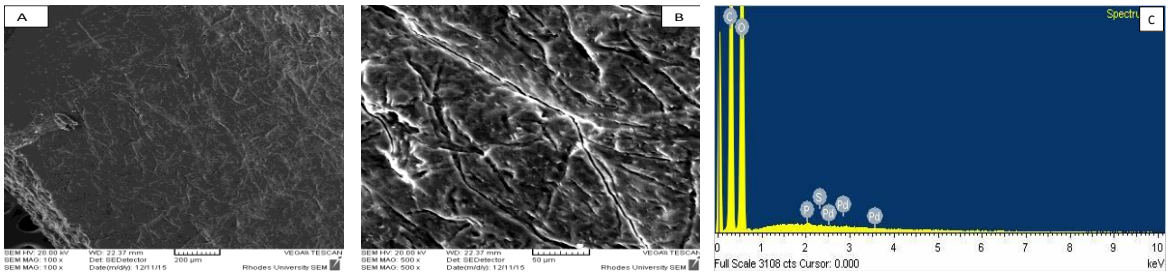

Fig. 9. (A) and (B) are SEM images of PdS3/potato starch nanocomposites. (C) EDS spectrum of the nanocomposites

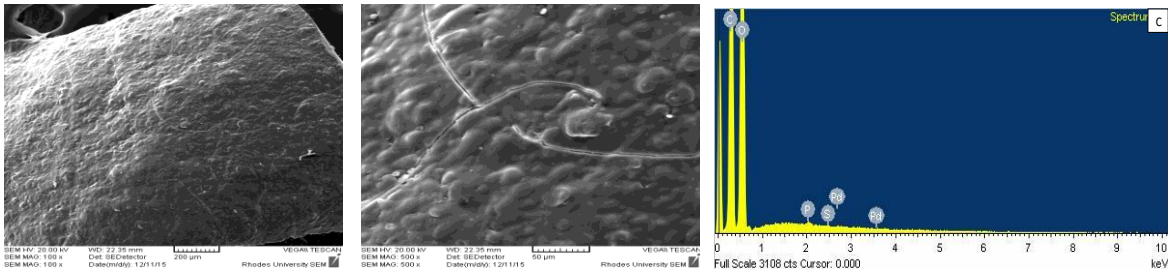

Fig. 10. (A) and (B) are SEM images of PdS4/potato starch nanocomposites. (C) is the EDS spectrum of the nanocomposites

Fig. 9 shows the SEM/EDS of PdS2/starch composites. SEM images show nanocomposites with increase in the roughness of surface morphology. PdS nanoparticles are well dispersed into the matrix of the starch. EDS shows peaks of Pd and S, which is the confirmation for the presence of nanoparticles. Figure 10 shows the SEM/EDS of PdS3/starch nanocomposites. The SEM images at low and high magnification show smooth composites with very few particles present. The EDS spectrun confirm the presence of metal sulfide nanoparticles with the presence of Pd and S elements. The SEM images shows smooth nanocomposites with few nanoparticles dispersed in the matrix of potato starch [46]. They have homogeneous surface morphology with close to spherical shapes. The EDS spectrum confirm the presence of PdS nanoparticles by peaks of Pd and S.

3.6 FTIR spectra studies of PdS/starch nanocomposites

The FTIR spectrum of PdS/potato starch nanocomposite shows impurities that might be due to the precursor used in the synthesis of PdS/potato starch nanocomposites. The broad peak at 3200 cm^{-1} can be ascribed to H_2O in the nanocomposites. Peaks around 1300 cm^{-1} are due to O-H deformation and C-C stretching of the ring. At 1000 cm^{-1} there is a sharp peak which can be attributed to O-C, C-C, and C-O deformations [47]. Around 1100 cm^{-1} there is a peak of C-O-C

and C-C stretching. The peak around 2900 cm^{-1} is small in the starch, but in the spectrum of nanocomposites, it is prominent because of the coordination of starch with nanoparticles [48].

4. Conclusions

In this study, we described the use of homoleptic Pd(II) dithiocarbamate complexes as single source precursor to synthesize PdS nanocrystals. The metal complexes were thermolysed in hexadecylamine (HDA) at 220 °C to prepare HDA-capped PdS nanoparticles. The as-prepared PdS nanoparticles dispersed in potato starch to prepare PdS/potato starch nanocomposites. The optical studies of the nanoparticles using electronic absorption and emission spectroscopy. showed that the absorption spectra of the PdS nanoparticles are blue shifted compared to their corresponding bulk materials indicating that the nanoparticles are quantum confined due to their small crystallite sizes while the photoluminescence spectra show narrow emissions that are red-shifted.

The XRD patterns confirmed the formation of cubic phase for PdS nanoparticles. TEM images of PdS showed monodisperse nanocrystal with average crystallite sizes of 6.94-9.62 nm for PdS1, 4.94-6.52 for PdS2, and 7-10.43 for PdS3. The TEM images shows individual PdS nanocrystals without any agglomeration. The SEM images showed uniform surface morphology of PdS nanoparticles with almost spherically shaped nanoparticles, while EDS confirms the presence of Pd and S for HDA-capped PdS nanoparticles respectively. SEM images and EDS of the PdS/potato starch nanocomposites confirmed the dispersion of the nanoparticles in starch matrices and their FTIR further confirms the formation of the nanocomposites.

Acknowledgements

We gratefully acknowledge the financial support of NRF and Sasol South Africa. AN acknowledge National Research Foundation/Sasol Inzalo Foundation innovation for the award of master scholarship.

References

[1] R.D. Tilley, D.A. Jefferson, J. Phys. Chem. B. **106**, 10895 (2002)
[2] M. Salavati-Niasari, G. Banaizan-Monfared, H. Emadi, M. Enhessar, C.R. Chimie. **16**, 929 (2013)
[3] Z. Li, J. Zhang, J. Du, T. Mu, Z. Liu, J. Chen, B. Han, J. Appl. Sci., **94**, 1643 (2004).
[4] R.M. Ma, X. L. Wei, L. Dai. H.B. Huo, G.G. Qin, Nanotech. **18**, 1, (2007).
[5] G. Fasol, Sci., **280**, 545 (1998).
[6] P.S. Nair, T. Radhakrishnan, N. Revaprasadu, G. Kolawole, P. O'Brien, J. Mater. Chem. **12**, 2722 (2002).
[7] R. Mahtab, J.P. Rogers, C.J. Murphy, J. Am. Chem. Soc., **117**, 9099 (1995).
[8] M. Nie, K.; Kai Sun, D.D. Meng, J. Appl. Phys. **106**, 054314 (2009)
[9] I.Y. Cha, M. Ahn, S.J. Yoo, Y. Sung, RSC. Adv. **4**, 38575 (2014).
[10] T. Ahn, J.H. Kim, H.M. Yang, J.W. Lee, J.D. Kim, J. Phys. Chem. C. **116**, 6069 (2012).
[11] R M. Alwan, Q.A. kadhim, K.M. Sahan, R.A. Ali, R.J.; Mahdi, N.A. Kassim, A.N. Jassim, Nanosci. Nanotech. **5**, 1, (2015).
[12] M.A. Malik, M.Y. Wani, M.A. Hashim, Arab. J. Chem. **5**, 397 (2012).
[13] H. Hasashi, Y. Hakuta, Materials, **3**, 3794 (2010).
[14] K. Ramasamy, M.A. Malik, J. Raftery, Dalton. Trans, **39**, 1460 (2010).
[15] V.K. Jain, J. Chem. Sci. **118**, 547 (2006).
[16) Y.C. Zhang, G.Y. Wang, X.Y. Hu, J. Alloys Compd. **437**, 47 (2007).
[17] P.A. Ajibade, B.C. Ejelonu, Spectr. Acta Part A: Mol. Biomol. Spectro. **113**, 408 (2013).
[18] M. Afzaal, M.A. Malik, P. O'Brien, Chem. Comm. 334 (2005).

[19] D.C. Onwudiwe, P.A. Ajibade, Int. J. Mol. Sci., **12**, 5538 (2011).
[20] T. Radhakrishnan, M.K. Georges, P.S. Nair, A.S. Luyt, V. Djoković, Colloid Polym Sci. **286**, 683 (2008).
[21] N. Moloto, N.J. Coville, S.S. Ray, M.J. Moloto, Physica B, **404**, 4461 (2009).
[22] Sh. Sohrabnezhad, A.J. Pourahmad, Alloys Compds, **505**, 324 (2010).
[23] A. Pourahmad, Sh. Sohrabnezhad, M.S. Sadjadi, K. Zare, Mater. Lett. **62**, 655 (2008).
[24] T. Radhakrishnan, M.K. Georges, P.S. Nair, A.S. Luyt, V. Djoković, Polym. Sci. **286**, 683 (2008).
[25] P.A. Ajibade, J.J. Osuntokun. Nanomater. **782526**, 1 (2014).
[26] L.D. Nyamen, V.S.R. Pullabhotla, A.A. Nejo, P. Ndifon, N. Revaprasadu, New J. Chem. **35**, 1133 (2011).
[27] J.Z. Mbese, P.A. Ajibade, J Sulf. Chem. **35**, 438 (2014).
[28] M.D. Regulacio, N. Tomson, S.L. Stoll, Chem. Mater. **17**, 3114 (2005).
[29] P.W. Dunne, C.L. Starkey, M. Gimeno-Fabra, E.H. Lester, Nanoscale, **6**, 2406 (2014).
[30] T.H. Larsen, M. Sigman, A. Ghezelbash, R.C. Doty, B.A. Korgel, J. Am. Chem. Soc. **125**, 5638 (2003).
[31] Z.A. Peng, X.G. Peng, J. Am. Chem. Soc. **124**, 3343 (2002).
[32] P.A. Ajibade, J.Z. Mbese, B. Omondi, Inorg. Nanomet. Chem. **47**, 202, (2017).
[33] T. Mthethwa, V.S.R. Pullabhotla, P.S. Mdluli, J. Wesley-Smith, N. Revaprasadu, Polyhedron, **28**, 2977 (2009).
[34] J.Y. Park, C. Aliaga, R.J. Renzas, H. Lee, G. Somorjai, Catal. Lett., **129**, 1 (2009).
[35] N.L. Botha, P.A. Ajibade, Mater. Sci. Semicond. Process. **43**, 149 (2016)
[36] G.K. Anderson, M. Lin, Inorg. Synth. **28**, 60 (1990).
[37] S. Wang, C. An, J. Yuan, Materials, **3**, 401 (2010).
[38] L.Z. Zhang, W. Sun, P. Cheng, Molecules **8**, 207 (2003).
[39] S. Dey, V.K. Jain, Plat. Met. Rev. **48**, 16 (2004).
[40] P. O'Brien, P. Waters, Chem. Vap. Deposition. **12**, 620 (2006).
[41] H.T. Boey, W.L. Tan, N.H.H. Abu Bakar, M. Abu Bakar, J. Ismail, J. Phys. Sci. **18**, 87 (2007).
[42] O. Masala, R. Seshadri, Annu. Rev. Mater. Res. **34**, 41 (2004).
[43] M.C. Tong, W. Chen, J. Sun, D. Ghosh, S. Chen, J. Phys. Chem. B. **110**, 19238 (2006).
[44] S.M.I. Morsy, Int. J. Curr. Microbiol. App. Sci **3**, 237 (2014).
[45] K. Prakobna, S. Galland, L.A. Berglund, J. Amer. Chem. Soc. **16**, 904 (2015).
[46] N. Kamellia, Z. Rezvanh, Chem. Centr. J. **6**, 23 (2012).
[47] M.A. Osorio, D. Restrepo, J.A. Velásquez-Cock, R.O. Zuluaga, U. Ursula Montoya, O. Rojas, P.F. Gañán, D. Marind, C.I. Castroe, J. Braz. Chem. Soc. **25**, 1607 (2014).
[48] K. Gipson, K. Stevens, P. Brown, J. Ballato, J. Spectrosc. **489162**, 1 (2015).